Integrated data analysis and end-to-end Simulations

Reijo Keskitalo
Lawrence Berkeley National Laboratory and University of California Berkeley

Introducing the session on Challenges of interdependencies in data analysis and end-to-end simulations: “Data analysis interdependencies”

Charge: *Describe "integrated data analysis" techniques, and the need for simulations required by such analysis*

Charge: *Describe "integrated data analysis" techniques, and the need for simulations required by such analysis*

Definition: I define integrated data analysis to involve

a) A module performing more than one analysis function in a single call

AND/OR

b) Set of modules that are iterated between to accomplish the analysis goal

LFI 2015 – a modular, non-integrated pipeline

Modular approach allows for parallel design, development and testing.

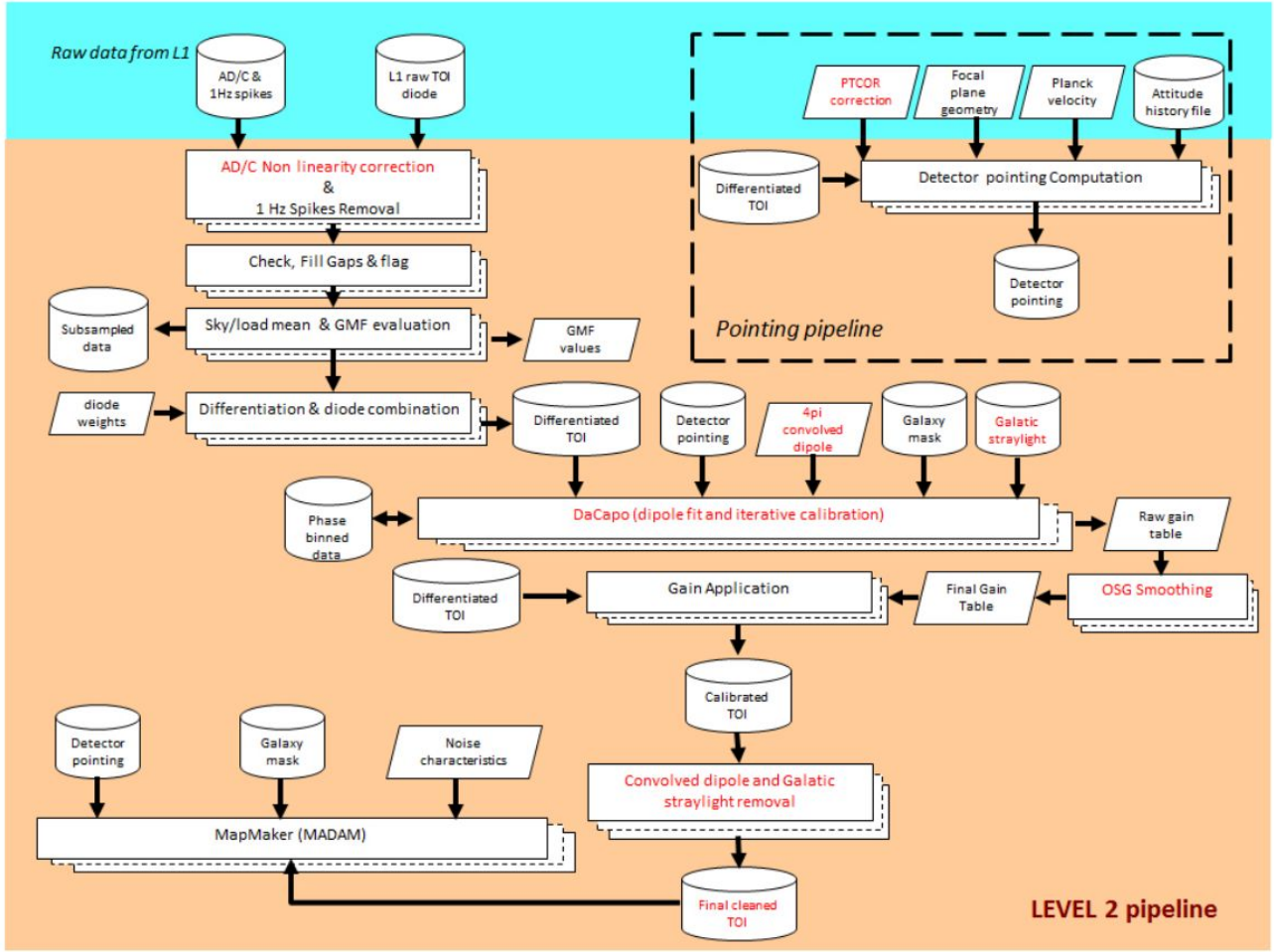

Fig. 1. Schematic representation of the Level 2 and pointing pipelines of the LFI DPC; elements in red identify those modified or augmented with respect to Planck Collaboration II (2014)

From *Planck 2015 results. II. Low Frequency Instrument data processing*

HFI 2015 – a modular, non-integrated pipeline

Highly modular pipeline

Even the “mapmaking” step separates into offset solution and map binning.

This was state-of-the art in 2015

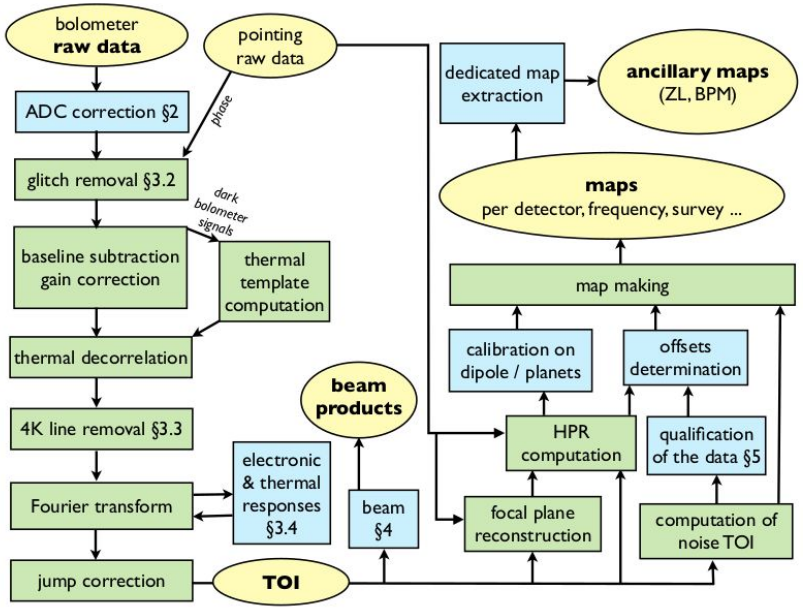

Figure 1. Schematic of the HFI pipeline. The left part of the schematic involves TOI and beams (this paper), while the upper-right part represents the map making steps (Paper 2). Ancillary maps are composed of zodiacal light templates (ZL) and polarization band-pass mismatch (BPM) maps. ADC = analogue-to-digital converter (see Sect. 2). HPR = `HealPix` ring (see Paper 2). “Beam products” refers to beam transfer functions, B_ℓ. Blue: changes in this release with section numbers corresponding to this paper. Yellow: released data products.

From *Planck 2015 results. VII. High Frequency Instrument data processing: Time-ordered information and beams*

Degenerate filters

- Unless the systematics are perfectly orthogonal, sequential template corrections can end up harming the data.
- Solution is obviously to orthogonalize the templates but that gets complicated if filters are applied in different spaces and/or the full pipeline is nonlinear
- If template amplitudes have physical meanings, orthogonalization reduces their S/N

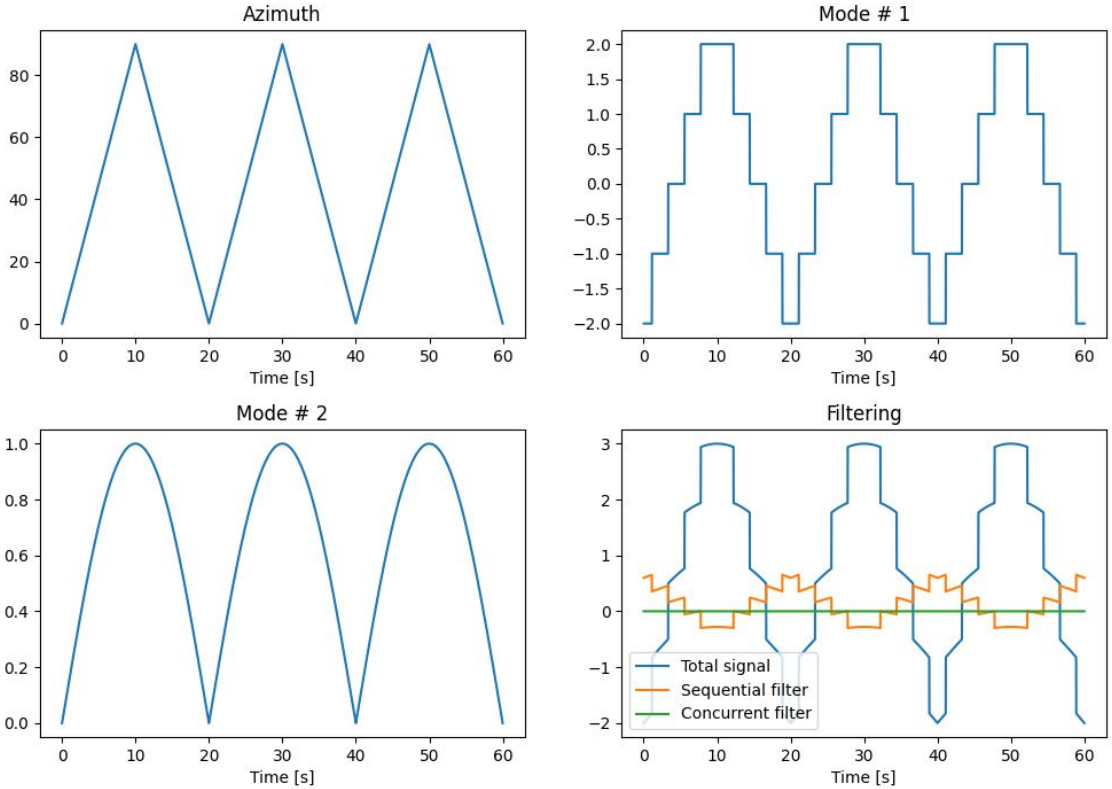

Original work

Degenerate modes

Planck 30GHz maps in 2015, 2018 and 2020 look very different.

How could each of them be self-consistent, yet so different?

30GHz PR3 - PR2

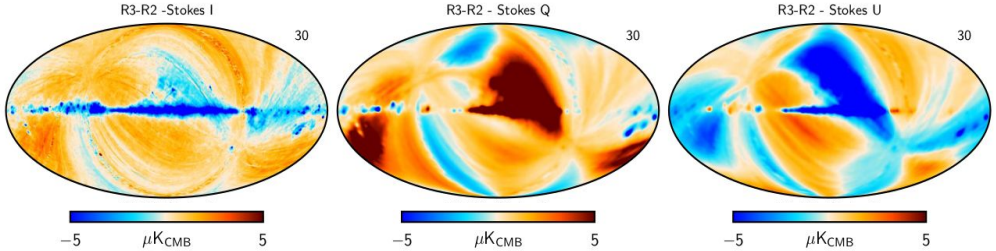

Fig. 13. Differences between 2018 (PR3) and 2015 (PR2) frequency maps in I, Q, and U. Maps are smoothed to 1° angular resolution for I and to 3° for Q and U, in order to highlight large-scale features. Differences are clearly evident at 30 and 44 GHz, and are mainly due to changes in the calibration procedure.

From *Planck 2018 results. II. Low Frequency Instrument data processing (2020)*

30GHz PR4 - PR3

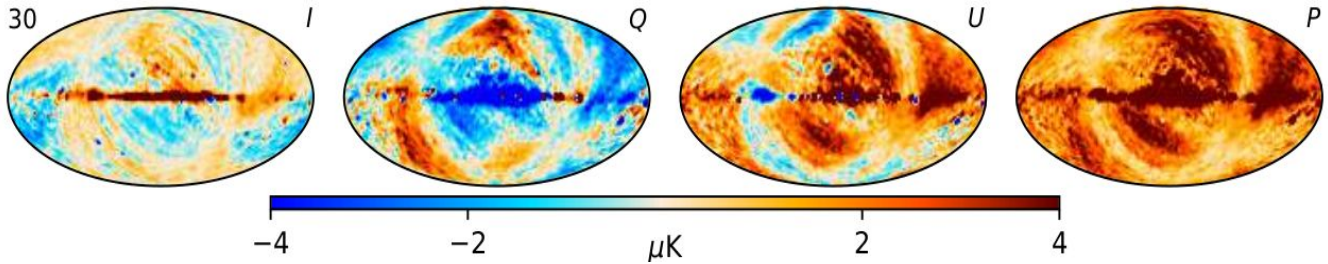

Fig. 42. NPIPE−2018 release difference maps in temperature and polarization. We have projected out the Solar dipole and zodiacal emission templates from the temperature differences, and performed a relative calibration using 50% of the sky to highlight differences beyond these trivial mismatch modes. All maps are smoothed with a 3° Gaussian beam to suppress small-scale noise.

From *Planck intermediate results LVII. Joint Planck LFI and HFI data processing (2020)*

Examples of integrated data analysis pipelines

- ArtDeco
- SRoll
- LFI PR3 processing with iterations over the sky model
- NPIPE
- BeyondPlanck

ArtDeco

- Keihänen & Reinecke (2012)
- Integrates 1/f noise mitigation, beam asymmetry mitigation and spherical harmonic expansion.
- Demonstrated on Planck LFI data
- Does not (yet) include bandpass mismatch correction

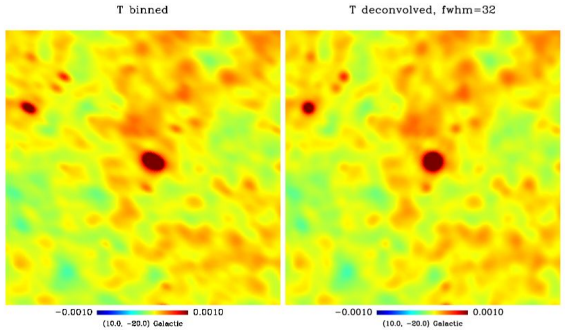

Fig. 4. Zoom into the 30 GHz temperature map without noise: binned (*left*) and deconvolved (*right*). Shown is a $1000' \times 1000'$ patch of the sky. The deconvolved map can be compared to the map constructed from the input $a_{T lm}$ (right panel of Fig. 2).

From *ArtDeco: a beam-deconvolution code for absolute cosmic microwave background measurements (2012)*

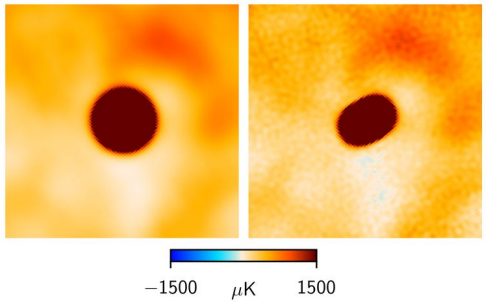

Fig. 2. A 10° patch around the Crab Nebula in the 30 GHz temperature map. *Left*: deconvolved. *Right*: PR3 30 GHz LFI map.

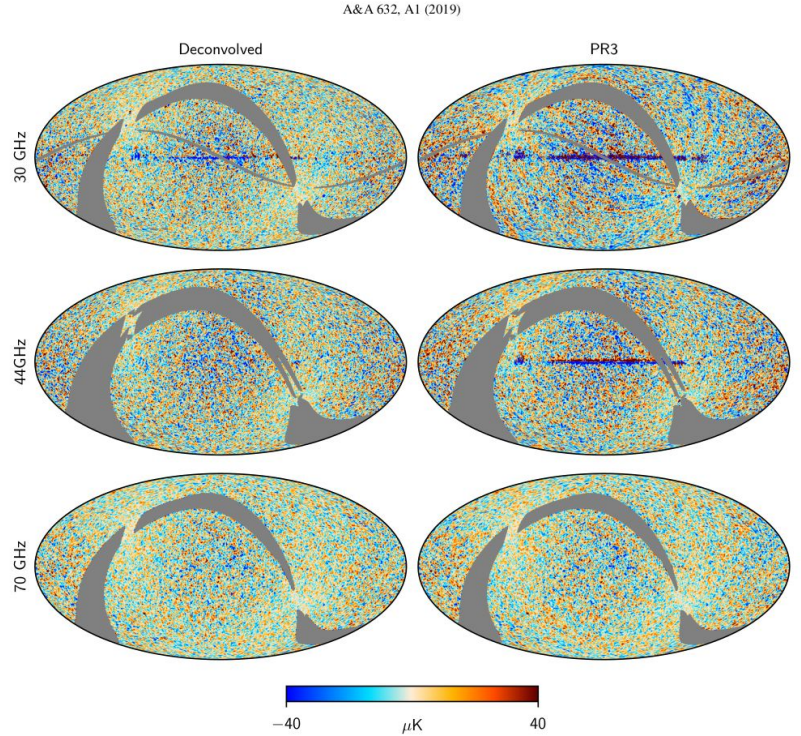

Fig. 4. Survey difference T maps S1 + S3 − S2 − S4. The maps are smoothed to 1° resolution. Deconvolution reduces beam shape residuals, revealing other signal residuals.

From *Beam-deconvolved Planck LFI maps (2019)*

PR3 (Legacy) – LFI/Commander iterations and SRoll

LFI calibration was shown to depend greatly on the quality of the sky model

Large scale polarization systematics in the PR2 data lead to development of an integrated data processing pipeline – an entirely new data reduction paradigm for Planck

As a result, PR3 delivered a significant improvement in large scale polarization systematics

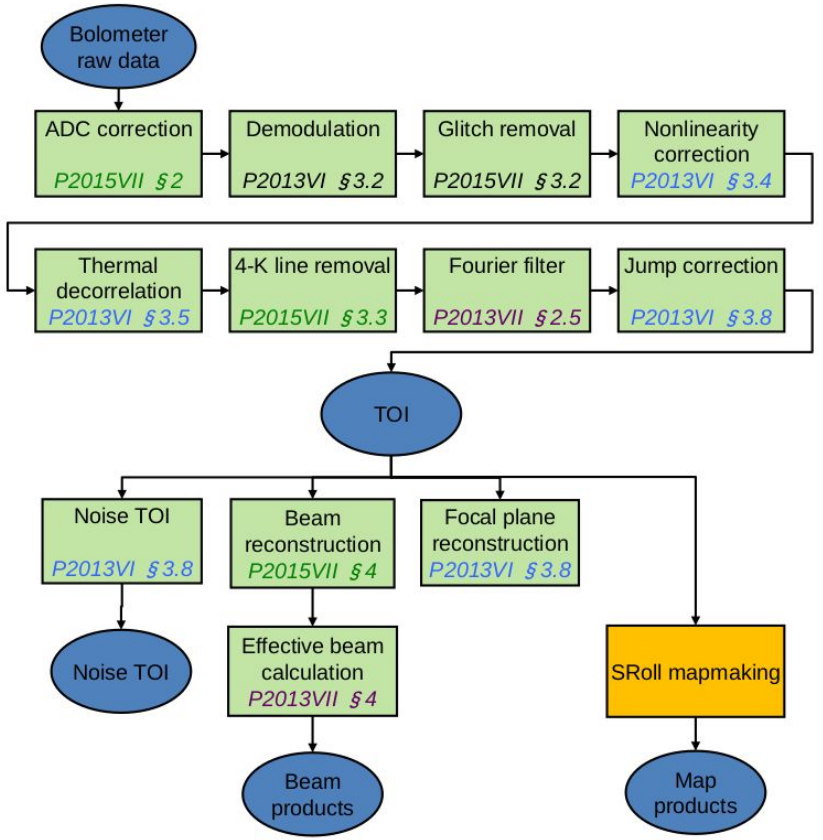

Fig. 1: Schematic of the HFI pipeline, referencing sections of previous papers (and this work) at each step.

From *Planck 2018 results. III. High Frequency Instrument data processing and frequency maps (2020)*

SRoll

Using full data and fitting for multiple systematics jointly maximizes the S/N

Fitting for gain makes the pipeline non-linear

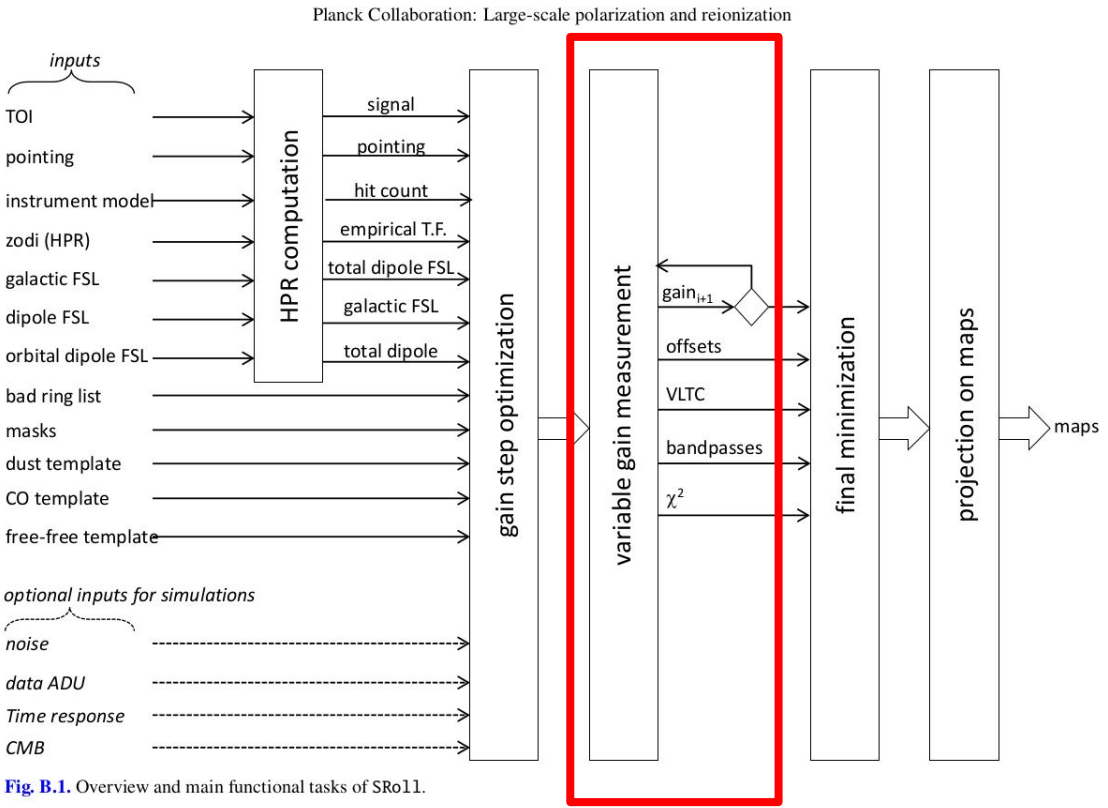

Fig. B.1. Overview and main functional tasks of SRoll.

From *Planck intermediate results XLVI. Reduction of large-scale systematic effects in HFI polarization maps and estimation of the reionization optical depth (2016)*

SRoll2

Delouis, Pagano, Mottet, Puget & Vibert (2019)

Replaces the gain fluctuation model for ADCNL with a well-motivated ADU-bias model (not a full model, as correction is applied to sample-integrated and demodulated data)

Significantly better parametrization of the ADCNL effect: captures signal distortion and is more orthogonal to other templates being fitted.

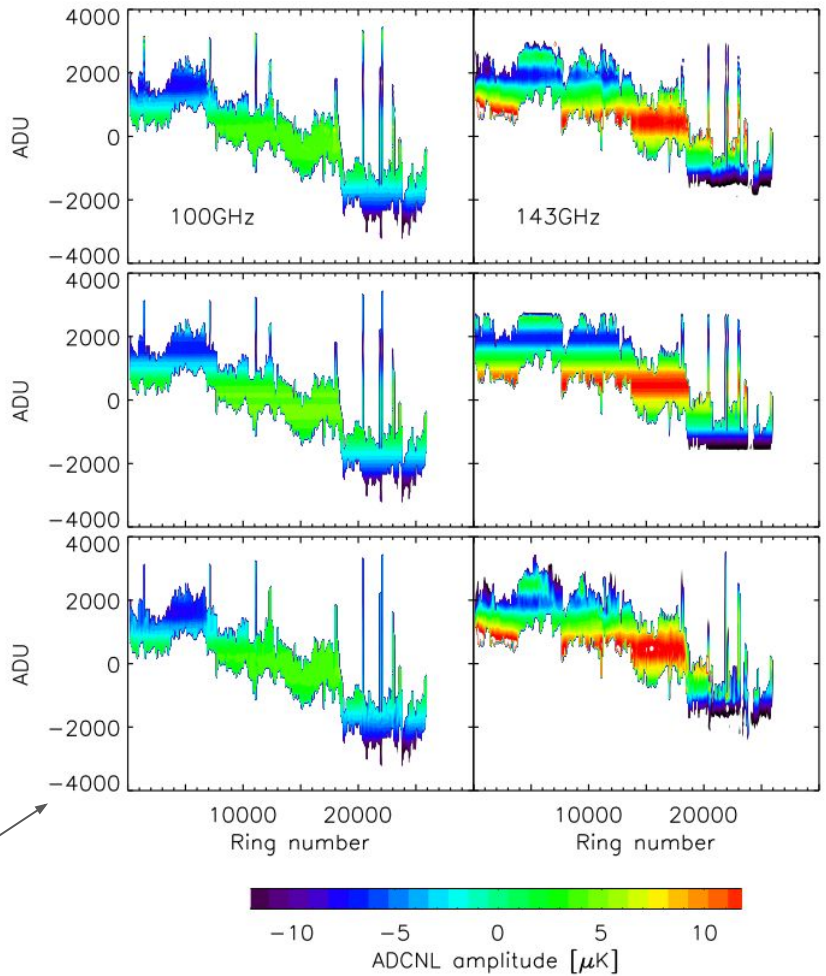

Fig. 3. Simulated ADCNL residuals (color coded) for the ADU level on the ADC (ordinate axis) along the time, expressed as ring number. Two bolometers are shown: left column for the 100-4b and right column for the 143-1a. First row: input of the simulation, second and third rows: their fitted 1D or 2D spline corrections without noise. Typical calibration is $\simeq 6\,\mu$K/ADU.

From *SRoll2 : an improved mapmaking approach to reduce large-scale systematic effects in the Planck High Frequency Instrument legacy Maps (2019)*

NPIPE

- NPIPE builds upon the integrated processing approach from LFI and HFI
- It adopts deep integration (several systematics at once) and ring-based processing from SRoll and leverages the additional information from multi-frequency sky modeling like LFI
- Just linear regression:
  d = Pm + Fa + n

Multi-frequency processing

1. Calibrate 30 and 353GHz
2. Calibrate 217GHz while fitting a 30/353GHz polarization model
3. Calibrate 44-143GHz while fitting a 30/217/353GHz polarization model

NPIPE template matrix example for 100-1a

Columns of the NPIPE template matrix visualized as pointing period vs. satellite spin phase.

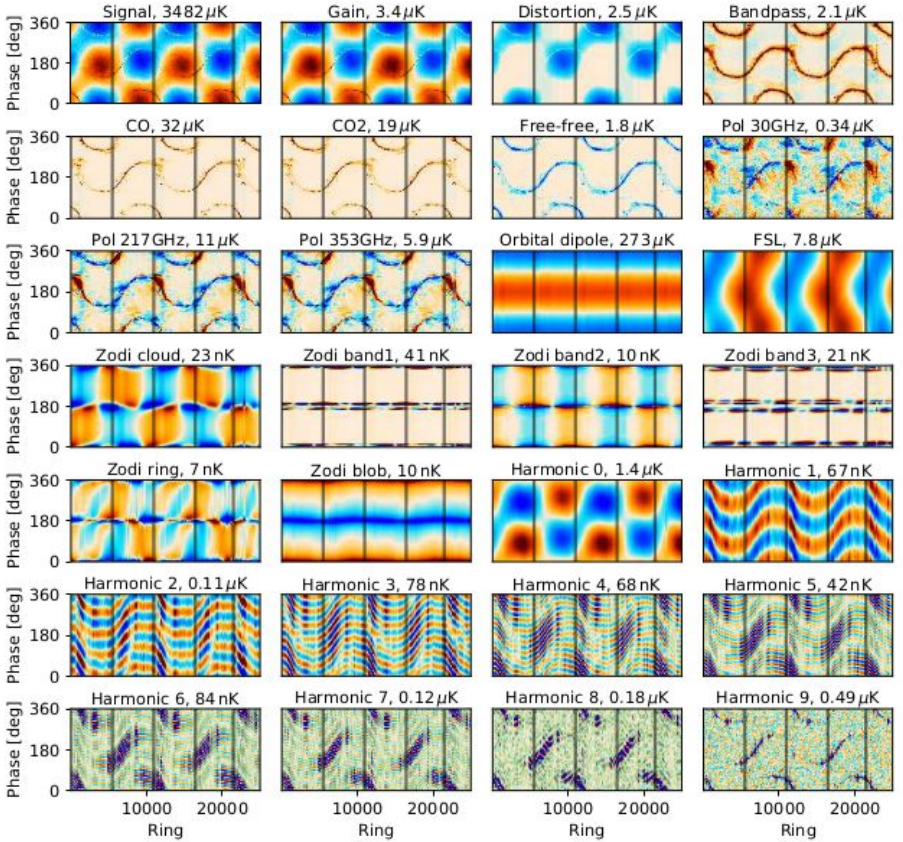

Fig. E.1. Signal and systematics templates for detector 100-1a, plotted as a function of pointing period (ring) and spacecraft spin phase. The gain and signal distortion templates are actually split into several disjoint steps that vary in length depending on the S/N. The templates for 100-1b are otherwise identical, but the 30, 217, and 353 GHz polarization templates are multiplied by −1. The far sidelobe (FSL) template is not fitted because of degeneracies, but it is estimated and subtracted. The polarization templates across all detectors share a single fitting amplitude. The zodiacal emission-template amplitudes are similarly shared. For 353 GHz and above, the harmonic templates are doubled to include frequency-dependent gain. At 100–217 GHz, only relative time-shift between frequency bins is modelled. The last harmonic template includes all frequencies not included in the other harmonic templates. The templates are scaled to match the rms amplitude of each systematic across the 100 GHz detectors, and the plotting ranges are chosen to match the 2σ range of each panel. To save space, the amplitude is reported in the title of each panel rather than as a colour bar. The grey vertical lines indicate the survey boundaries. Figure E.2 shows `HEALPix` maps of these templates that include only the first survey.

From
Planck intermediate results LVII. Joint Planck LFI and HFI data processing (2020)

PR4 - PR3

PR4 - SRoll2

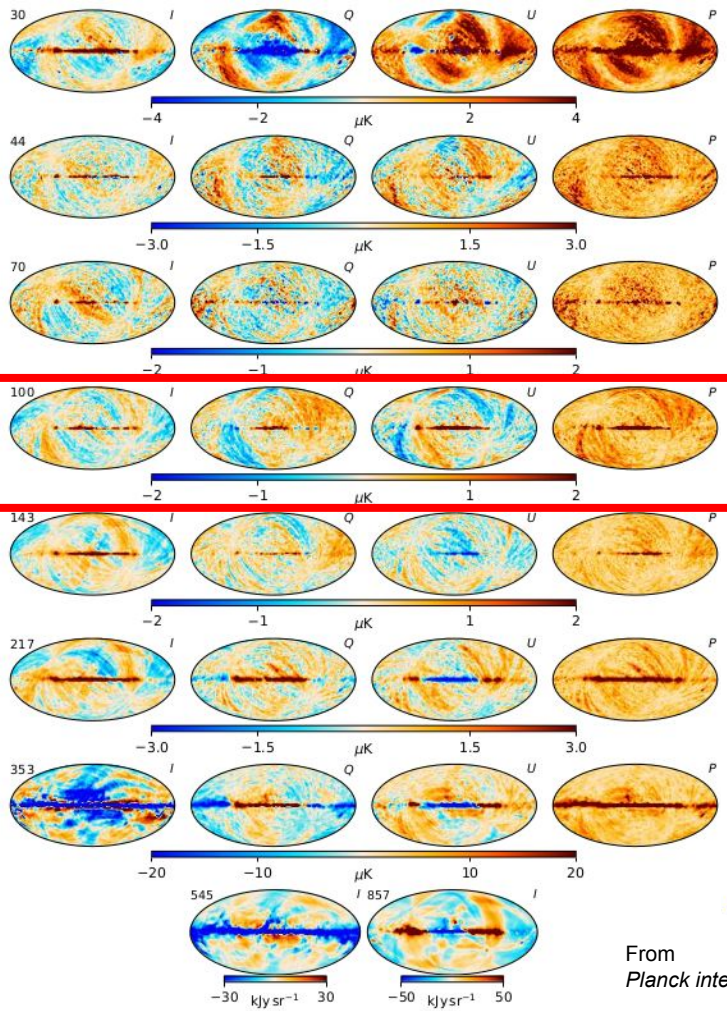

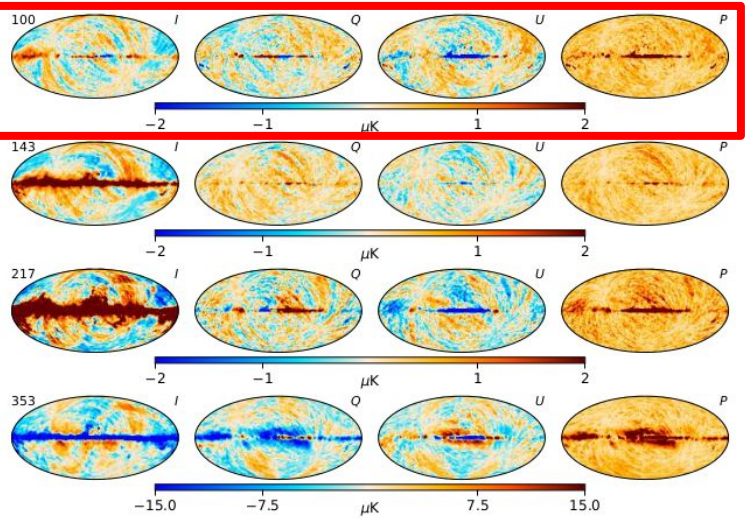

Fig. 44. NPIPE−SRoll2 difference maps in temperature and polarization to compare to Fig. 42.

From
Planck intermediate results LVII. Joint Planck LFI and HFI data processing (2020)

Fig. 42. NPIPE–2018 release difference maps in temperature and polarization. We have projected out the Solar dipole and zodiacal emission templates from the temperature differences, and performed a relative calibration using 50% of the sky to highlight differences beyond these trivial mismatch modes. All maps are smoothed with a 3° Gaussian beam to suppress small-scale noise.

PR4 - PR3

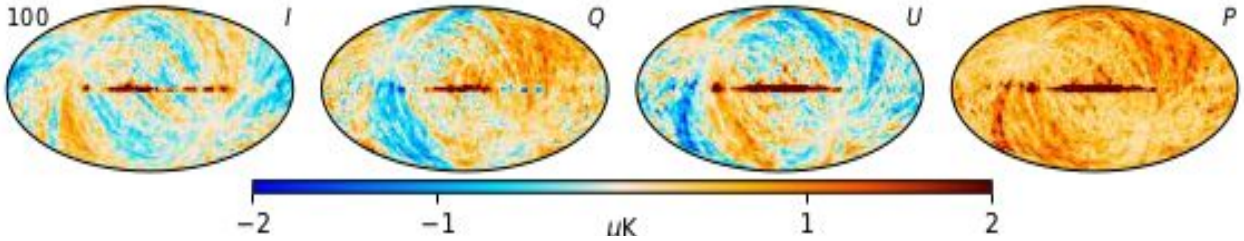

PR4 - SRoll2

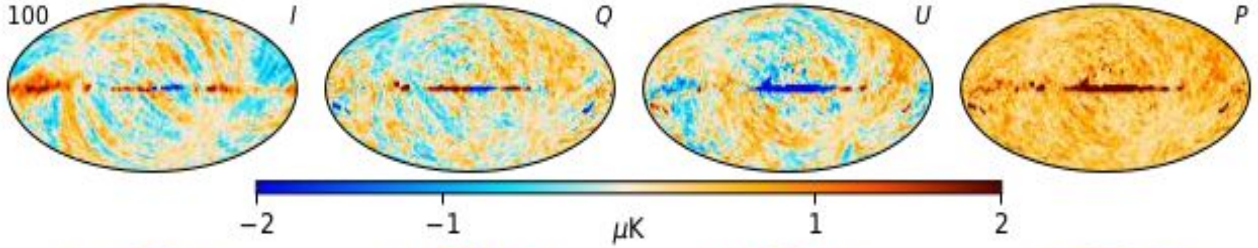

From
Planck intermediate results LVII. Joint Planck LFI and HFI data processing (2020)

Noise bias

Additional data, reworked deglitch, new noise weights, short baseline destriping and the polarization prior suppress noise at all angular scales.

Green bias spectra are intermediate spectra that haven't been corrected for pipeline transfer function.

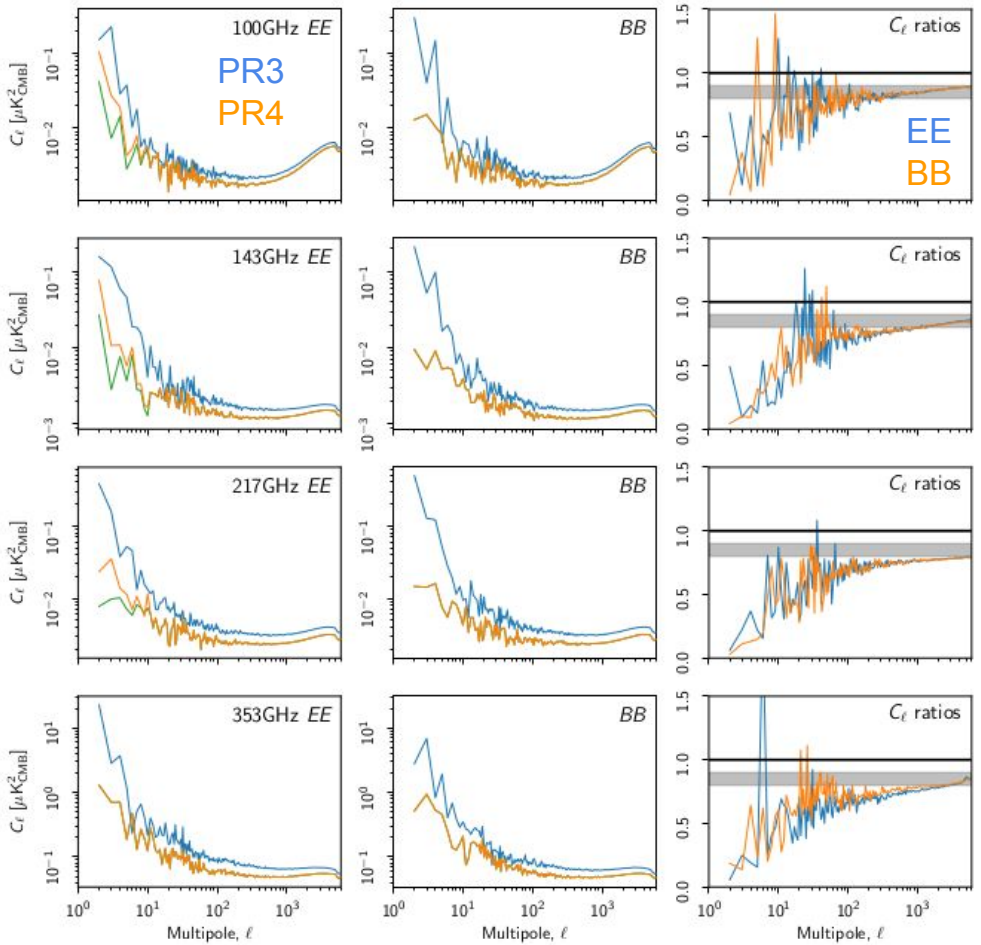

Fig. 40. *EE* and *BB* detector-set difference power spectra. The *first two columns* show PR3 (blue), raw NPIPE (green), and transfer-function-corrected NPIPE (orange) null-map power spectra. Note that PR3 detector sets are *not* the same as were differenced for Fig. 14 in Planck Collaboration III (2020), but rather ones that were destriped independently. The *third column* of panels shows the transfer-function-corrected NPIPE/2018 *EE* and *BB* ratios in blue and orange, respectively. NPIPE has notably less power at all angular scales. The grey band in the third column indicates a 10–20% improvement in power. These spectra are computed over 50.4% of the sky, corrected for the sky fraction and binned into 300 logarithmically-spaced bins. The polarization amplitudes of 2015, 2018, and NPIPE detector-set difference maps are shown in Fig. 39.

From *Planck intermediate results LVII. Joint Planck LFI and HFI data processing (2020)*

Polarization prior

Disabling the noise prior increases the NPIPE noise bias to match the PR3 noise level at large scales.

No change at ell > 100.

Red curves show the NPIPE noise bias without the polarization prior.

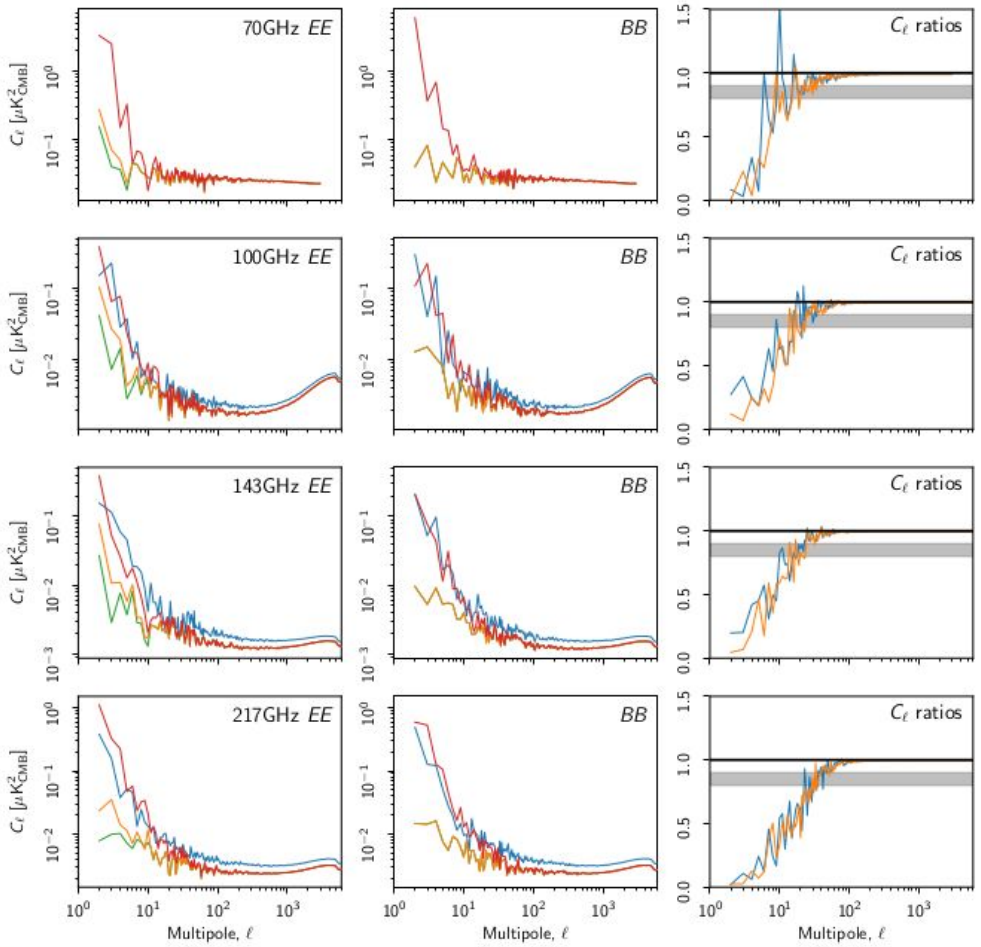

Fig. 41. Effect of the polarization prior on *EE* and *BB* detector-set difference power spectra. For 100–217 GHz, the green, orange, and blue lines on the *EE* and *BB* plots are the same as in Fig. 40 but here we add a red line, showing the power spectra for an alternative version of the NPIPE detector-set maps that are computed *without* the polarization prior. There is no blue line at 70 GHz because there is no comparable detector-set split in PR3, and 353 GHz is not shown because it is always calibrated without the polarization prior.

From *Planck intermediate results LVII. Joint Planck LFI and HFI data processing (2020)*

BeyondPlanck

From TOD to a sky model and everything in between

Use external data to overcome degeneracies and poorly constrained modes

Separate talk by Mathew Galloway immediately after this!

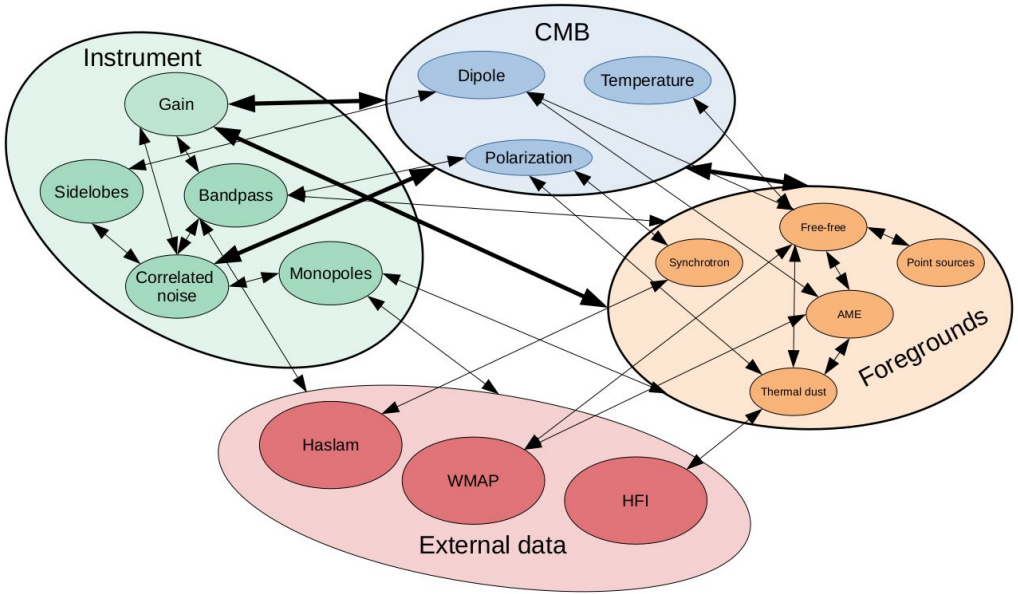

Fig. 8. Schematic overview of the primary parameters and external data sets considered in the current BeyondPlanck analysis and their inter-dependencies. This chart is intended to visualize the deeply integrated nature of a modern CMB analysis problem; changing any one of these parameter can lead to significant changes in a wide range of other parameters, and tracing these joint uncertainties is critically important for high-precision experiments.

From *BeyondPlanck I. Global Bayesian analysis of the Planck Low Frequency Instrument data (2022)*

Address the various ways to approach issues such as

- Cleaning
- Calibration
- Systematics
- instrument characterization
- foreground removal
- CMB characterization and
- parameter estimation

in a combined manner

Integrated data analysis for CMB-S4 and LiteBIRD

- Pros and cons
  - Different development models
  - Correlated errors
  - More complicated interpretation of template amplitudes
  - “Black Box”
- Feasibility
  - Requires all or a lot of data at once
  - Resource intensive, no batch processing
  - Degeneracies may prevent integrated analysis

Charge: *What are the challenges associated with the production and utilisation of simulations which are critical for the next generation of CMB datasets?*

Mission Scale Simulations

Large scale simulations require large scale preparation (months if not years):

- Sky model
  - prepare for optimistic, pessimistic and realistic cases
- Instrument model
  - Always up to date
  - Start with best guesses but don’t oversimplify. Develop the database and simulation modules for the general case
- Observation model
  - Needs sufficient realism, can become an extremely useful tool in mission planning and forecasting
- Data analysis pipeline
  - Must optimize! Needs to run 1,000 times, not just once
  - Certain systematics may be difficult or overly expensive to simulate. It may suffice to simulate residuals
- Validate, execute, verify and review. Never forget a lesson learned.

Examples of end-to-end simulations

PR2/FFP7 - 10,000 realizations but significant noise mismatch

PR3/FFP10 (also SRoll2) - (almost) true E2E but with noise mismatch

PR4/NPIPE - not true E2E but much improved noise match

Food for thought:

Where to perform noise estimation and how? What are the primary degrees of freedom? Physical or effective model of the detector?

How to include systematics? Is it enough to include the fitting and removal or does the systematic need to be implemented?

If your pipeline is fully integrated, every simulation is E2E!

PR2/FFP7 (1/2)

Largest Planck simulation set ever published.

10,000 noise and CMB realizations.

Missing large scale polarization systematics and half ring correlated noise

CMB foregrounds noise

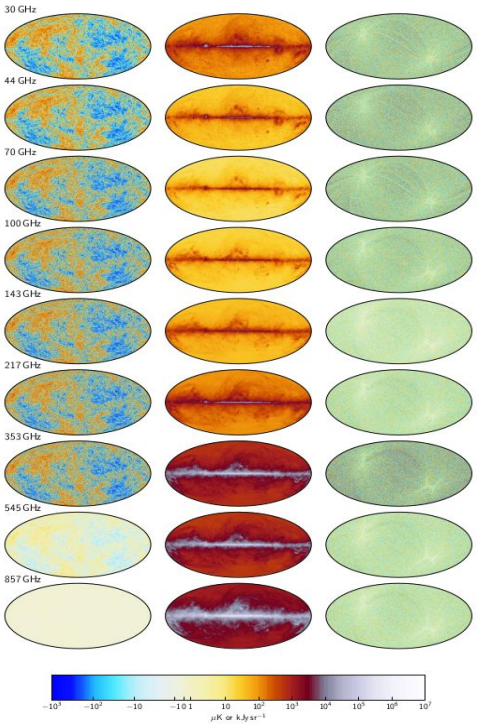

Fig. 12. Left to right, the baseline FFP8 fiducial CMB, foreground and noise component temperature channel/mission/full maps at each frequency. Frequencies 30–353 GHz are plotted in μK, while 545 and 857 GHz are plotted in kJy sr^{-1}. See Fig. 16 for the combined temperature maps.

Polarization amplitude:
Flight vs. simulation

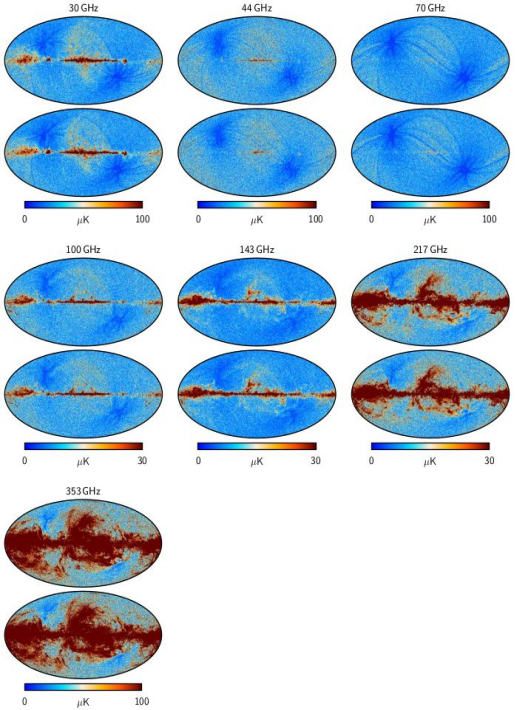

Fig. 17. Pairs of channel/mission/full total polarization maps, comparing FFP8 simulations (upper) and 2015 *Planck* (lower) data. All maps are downgraded to $N_{side} = 256$.

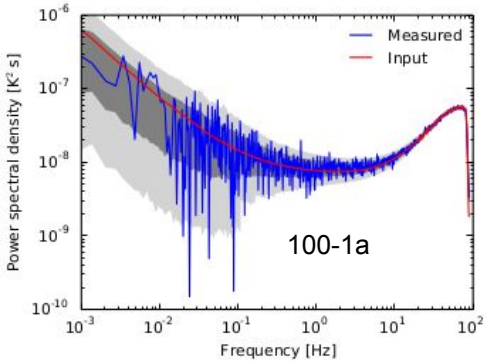

Fig. 3. Example comparison of the input and recovered noise PSDs for one pointing period of a signal+noise simulation of HFI bolometer 100-1a. The shaded regions around the input model reflect the asymmetric realization scatter of the estimated PSDs at 68 % and 95 % confidence intervals in each of the 707 logarithmically-placed frequency bins.

From *Planck 2015 results. XII. Full Focal Plane simulations (2016)*

PR2/FFP7 (2/2)

Half ring, half difference null maps, BB spectrum

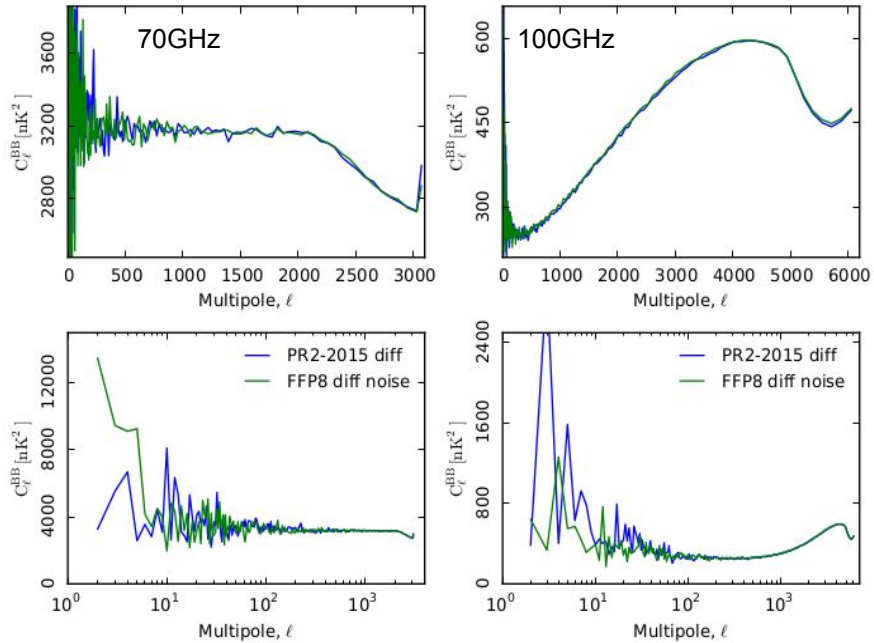

Fig. 4. *BB* spectra of 70 GHz (*left*) and 100 GHz (*right*) half-ring half difference noise maps, for both FFP8 simulations (*green*) and flight data (*black*). Differences at the low-ℓ end are caused by sample variance. These are pseudo-spectra, computed on 75 % of the sky with the Galactic plane and point sources masked. *Top:* Linear horizontal axis to show small-scale behaviour. *Bottom:* Logarithmic horizontal axis to show large-scale behaviour.

Full frequency map BB spectrum

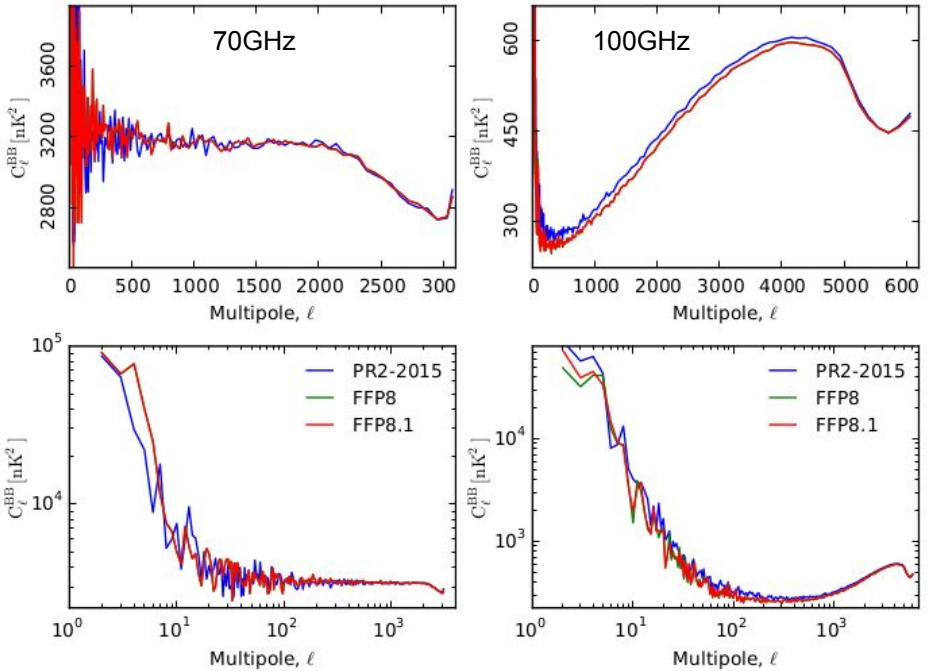

Fig. 18. Comparison of the *BB* spectra of the channel/mission/full simulated and flight data maps using pseudo-spectra computed on 75 % of the sky with the Galaxy and point sources masked, showing excellent agreement at 70 GHz but a few percent discrepancy at almost all angular scales at 100 GHz. *Left*: 70 GHz full map *BB*-spectra. *Right*: 100 GHz full map *BB*-spectra. *Top*: Linear horizontal axis shows small scale behaviour. *Bottom*: Logarithmic horizontal axis shows large scale behaviour.

From *Planck 2015 results. XII. Full Focal Plane simulations (2016)*

PR3/FFP10

PR3 HFI simulations (aka FFP10) are the purest end-to-end simulation set released for Planck

They propagate the signal from raw bolometer data down to ADCNL and bandpass-corrected frequency maps.

Expensive deglitching is skipped. No 4K lines.

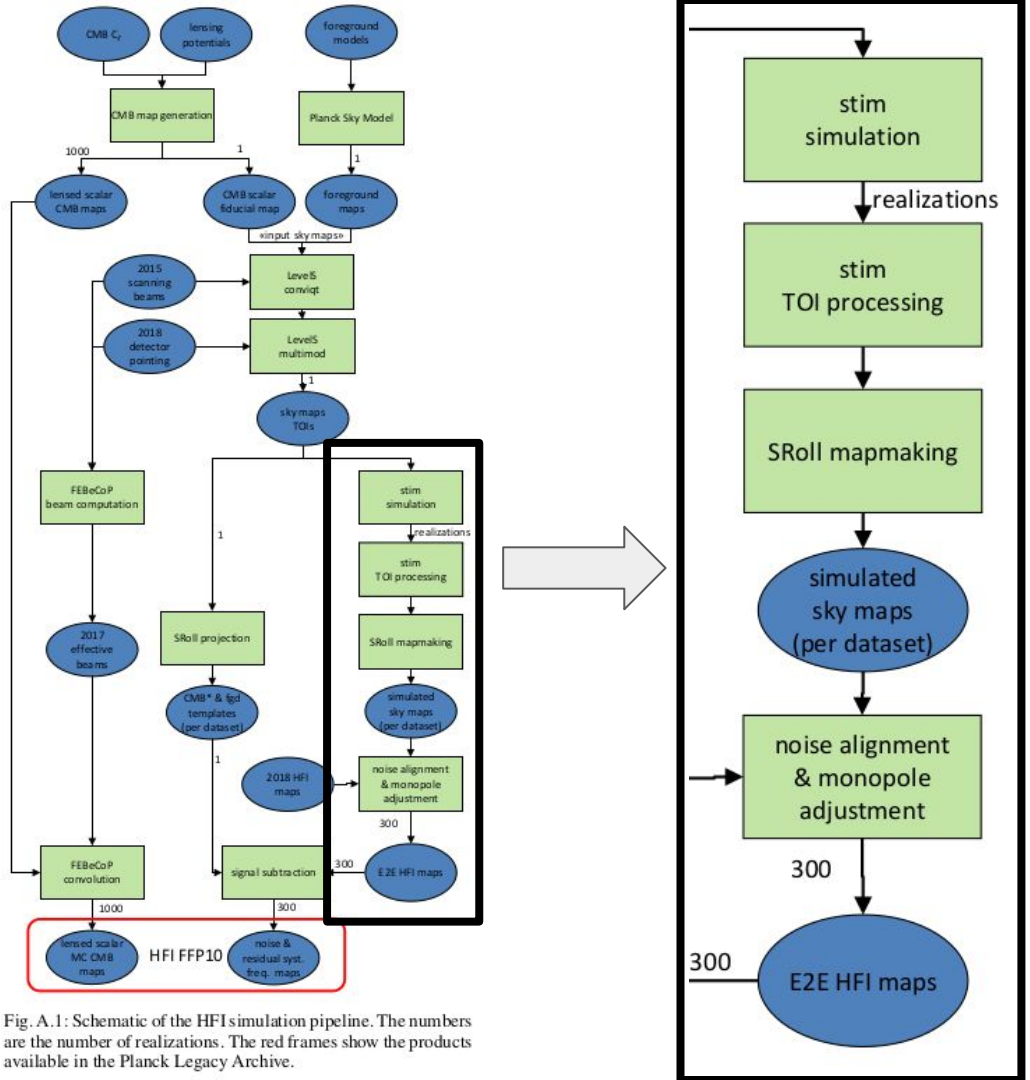

Fig. A.1: Schematic of the HFI simulation pipeline. The numbers are the number of realizations. The red frames show the products available in the Planck Legacy Archive.

From *Planck 2018 results. III. High Frequency Instrument data processing and frequency maps (2020)*

PR3/FFP10

PR3 HFI simulations (aka FFP10) are the purest end-to-end simulation set released for Planck

They propagate the signal from raw bolometer data down to ADCNL and bandpass-corrected frequency maps.

Expensive deglitching is skipped. No 4K lines.

Simulating noise in the raw bolometer model left a mismatch between real and simulated maps requiring map domain noise-alignment. Significant mismatch persisted after the alignment.

Real / simulated CMB map power spectrum ratio, PR3, PR4

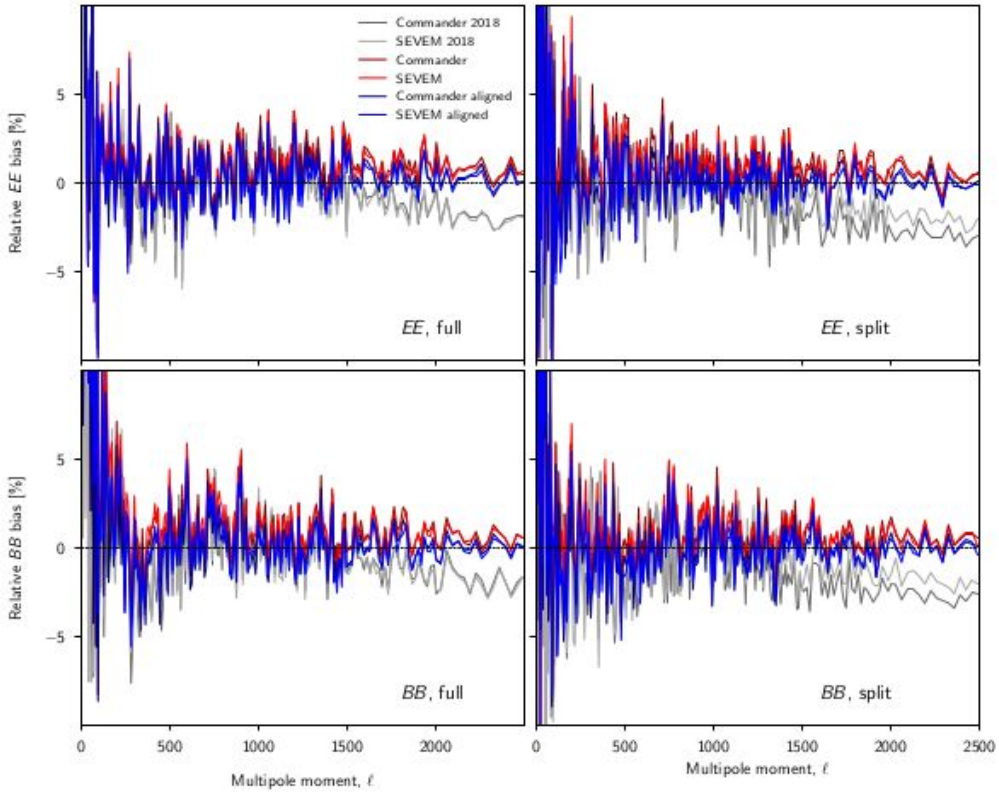

Fig. 73. Power spectrum consistency between the foreground-cleaned Commander (dark curves) and SEVEM (light curves) CMB polarization map and corresponding end-to-end-simulations. Each panel shows the fractional difference between the angular power spectrum computed from the observed data and the mean of the simulations. Blue and red curves show results derived for NPIPE data using simulations *with* and *without* noise alignment, respectively, while grey curves show similar results derived from *Planck* 2018 data using simulations *with* noise alignment. Rows show results for *EE* (*top*) and *BB* (*bottom*) spectra, while columns show results for full-mission (*left*) and split (*right*) data. In the latter case, A-B split results are shown for NPIPE, while half-mission splits are shown for *Planck* 2018.

From *Planck intermediate results LVII. Joint Planck LFI and HFI data processing (2020)*

PR4 (NPIPE)

Limit the simulation to the “reprocessing” step equivalent to SRoll in PR3.

Convolve each CMB realization with actual scanning beams

Add the Commander sky model with measured bandpass mismatch

For LFI, add (smoothed) measured gain fluctuations

Use the FFT technique to simulate the instrumental noise with measured PSD and correlation.

No added ADCNL or transfer function errors – only simulate the template fitting uncertainty and associated errors

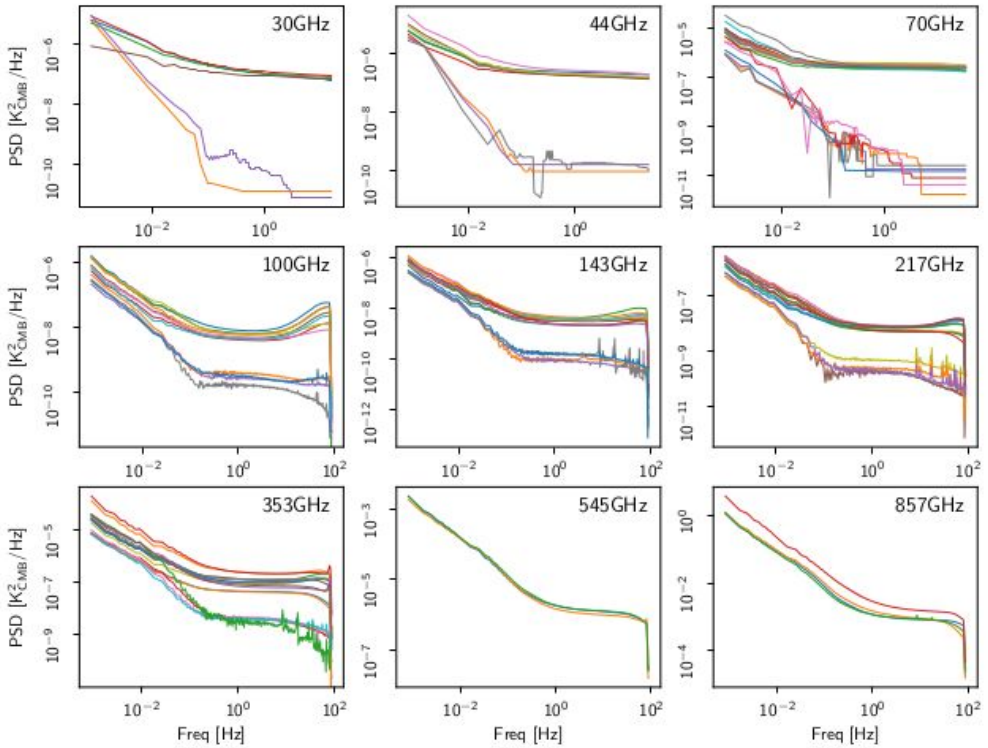

Fig. 27. Averaged noise PSDs for each detector (upper curves) and correlated-noise modes for each polarized horn (lower curves). The total noise power is the sum of the correlated and uncorrelated modes. These noise PSDs are measured from the data by subtracting a signal estimate and then evaluating the sample-sample covariance function. The HFI noise is suppressed near the Nyquist frequency (≈90 Hz) by the bolometric transfer function filtering. The PSDs are used for simulating the $1/f$ noise fluctuations, and as inputs to the Madam noise filter for destriping.

From *Planck intermediate results LVII. Joint Planck LFI and HFI data processing (2020)*

Summary

Planck demonstrated the power of integrated data analysis.

This was not by design but by necessity.

Modular approaches are probably more intuitive. Integrated analysis is **challenging** when the data contain unknown or poorly understood features.

Nevertheless, when S/N is of the essence, only an integrated analysis will make use of the full statistical power of the experiment.

Full E2E simulations present an entirely different level of requirements for code optimization and computing resources.